Polymers in Shear Flow near Repulsive Boundaries

Edgardo Duering and Yitzhak Rabin*

Department of Chemical Physics, Weizmann Institute of Science, Rehovot 76100, Israel.
Received August 29, 1989; Revised Manuscript Received October 25, 1989

ABSTRACT: We report the results of computer simulations of polymers with excluded-volume interactions, in simple shear flow between impenetrable walls. The projections of the polymer radius and the end-to-end distance along and perpendicular to the flow direction, the monomer and center of mass distributions, and the surface excess are studied as a function of the distance from the wall. Contrary to recent evanescent wave-induced fluorescence studies, we find that the width of the depletion layer near the wall decreases with increasing shear rate. Possible reasons for the discrepancy are discussed.

1. Introduction

Extensive literature exists on polymer solutions in homogeneous unbounded flows, where one may assume that the polymer concentration is everywhere uniform.[1] Much less is understood about polymer behavior in inhomogeneous flows where one might expect gradients in the polymer concentration profile, due to either the position dependence of the velocity gradients in bulk flow[2,3] or due to the presence of boundaries.[4] While the former case occurs in many important flows where macroscopically observable effects are produced, the latter effects are more subtle and involve concentration inhomogeneities on length scales comparable to polymer dimensions. Since these length scales are typically smaller than the wavelength of visible light, they cannot be probed by standard optical techniques. The direct observation of such phenomena became possible only recently, with the advent of new experimental techniques, such as the evanescent wave-induced fluorescence (EWIF) method, that can probe the polymer concentration profile in the depletion layer adjacent to the walls.[5] The unexpected findings of shear-induced thickening of the depletion layers[6] provoked our initial interest in this problem.

In this work we study the conformations and the concentration profiles of two-dimensional polymers in good solvents, subjected to simple shear flow between repulsive walls. Since there is no analytical solution even for the equilibrium (no flow) problem of polymers with excluded volume, in the presence of a wall, we have to resort to computer simulations. The calculations were performed on the Convex computer at the Weizmann Institute of Science (Rehovot, Israel). The model used in the simulations is described in section 2. In order to test the model and the computer code, the Monte Carlo (MC) algorithm is applied to the equilibrium problem of unbounded polymer solutions in good and Θ solvents (with and without excluded volume, respectively), in section 3. Good agreement is found between our simulation and the analytical (exact) results for the exponents of the radius of gyration, the end-to-end distance, and the relaxation time. The case of polymers in good solvents, confined to move between two parallel repulsive walls, is studied in section 4. The monomer and center of mass distributions, the projections of the radius of gyration parallel and perpendicular to the flow direction, and the surface excess are studied, first in equilibrium and then in the presence of simple shear flow. The main findings are the existence of shear-dominated bulk and wall-dominated boundary regions and the shear-induced narrowing of depletion layers. These results are discussed in section 5 and are compared with recent observations of shear thickening of the depletion layers.[6] Possible reasons for the observed discrepancy are also considered.

2. Model

The polymer consists of N spherical monomers, each one of radius $b = 0.5$. Monomers are free to move, subject to the following constraints: the maximum distance between nearest neighbors along the chain contour is d_{max}, and the minimum distance between any pair of monomers is d_{min}. We take $d_{min} = 0$ in the absence of excluded-volume effects and $d_{min} = 1$ when these effects are included.[7] d_{max} is close to 2 and will be discussed later. Since the constraints can be replaced by a hard-core effective potential that does not introduce an energy scale into the problem, the results are independent of temperature and the free energy is of entropic origin. Such a potential generates small persistence lengths, and good agreement with asymptotic (e.g., $N \to \infty$) results is expected for reasonably small values of N. Another advantage of this potential lies in the simplicity of the MC procedure, since the statistical weights (Boltzmann factors) are 0 or 1 for forbidden and allowed moves, respectively.

In the absence of shear we sample the configuration space using the Brownian dynamics method:[8] we choose a monomer at random and attempt to update its location by adding a vector of fixed length s and randomly chosen direction to its current position. This process is then repeated N times during a "MC time unit" that is taken to be the unit time in the calculations. Since an attempted move is accepted only if the new position of the monomer is allowed by the potential, the acceptance rate p is different with and without excluded-volume effects. This acceptance rate depends on the step length s and does not tend to unity when $s \to 0$, owing to the finite values of d_{max} and d_{min} (the latter nonvanishing only in presence of excluded-volume interactions), but gets close to it. For a single isolated monomer this algorithm generates Brownian motion with a diffusion coefficient $D_0 = ps^2/4$. The diffusion constant of the whole polymer is thus $D = D_0/N = ps^2/4N$. In order to prevent the polymer from crossing itself in the presence of excluded-volume interactions, via processes in which a monomer "squeezes" through the space between two other, nearest-neighbor monomers, s was chosen to satisfy $s^2 < 4 - d_{max}^2$.

The above procedure is a simplified version of the general Brownian dynamics algorithm. It satisfies the detailed balance conditions,[8] and therefore we may expect that after a sufficient time the polymer approaches equilibrium.

We perform the MC simulation for a polymer of N monomers with $5 \le N \le 40$ and evaluate the root-mean-

0024-9297/90/2223-2232$02.50/0

square (rms) end-to-end distance

$$R_{1n} = \langle (x_N - x_1)^2 + (y_N - y_1)^2 \rangle^{1/2} \quad (2.1)$$

and the radius of gyration

$$R_g = \frac{1}{N} \langle \sum_{i=1}^{N} ((x_i - x_{cm})^2 + (y_i - y_{cm})^2) \rangle^{1/2} \quad (2.2)$$

where $[x_{cm}, y_{cm}]$ is the position of the center of mass.

If $G(R)$ is some property that depends on the instantaneous configuration of the polymer $\{R(t)\}$, then the autocorrelation function of G is defined as

$$C_N(G(t)) = \frac{\langle G^*(t_0)G(t_0+t) \rangle - |\langle G(t_0) \rangle|^2}{\langle |G(t_0)|^2 \rangle - |\langle G(t_0) \rangle|^2} \quad (2.3)$$

The correlation functions of R_{1n} and R_g were evaluated for different values of N and were observed to decay exponentially

$$C_N(G(t)) = \sum a_i e^{-(t/\tau_i)} \quad (2.4)$$

in agreement with the Rouse model.

Although there is some ambiguity in the definition of the polymer correlation time, different choices involve different prefactors and do not affect the exponents. We define the correlation time as the time it takes for the center of mass of a polymer to diffuse over a distance equal to its radius of gyration, R_g

$$\tau = R_g^2/D = 4R_g^2 N/ps^2 = t_0 N^{1+2\nu} \quad (2.5)$$

where t_0 is a proportionality constant, and we assume that $R_g \propto N^\nu$, where ν is the excluded-volume exponent.

The computation time is now estimated as follows: because the MC procedure generates a highly correlated sequence of configurations, the time required to obtain independent sample configurations has to be of the order of the correlation time. As the correlation time increases as $\tau = t_0 N^{1+2\nu}$ and as there are N monomers in each polymer, without excluded-volume interactions, $\nu = 0.5$, and the computation time increases as $t_0 N^3$. With excluded-volume interactions, $\nu = 0.75$, and, in addition, each attempt to move a monomer requires N excluded-volume checks with other monomers. This leads to computation time $t_0' N^{4.5}$, where t_0' can be different from t_0.

3. Monte Carlo Simulation

In order to prevent the polymer from crossing itself in the presence of excluded-volume interaction, the step length s and the maximum possible distance between nearest neighbors were set at $s = 0.35$ and $d_{max} = 1.97$. For $5 \le N \le 40$ this gives a rejection rate of $0.3 < 1 - p < 0.4$ due to constraints associated with d_{max} $(1 - p \simeq 0.25)$ and d_{min} $(1 - p \simeq 0.10)$, where the rejection rate is defined as the probability that a monomer does not execute a move since such a move would violate the model constraints. These numbers were checked during the simulations to make sure that one is not trapped in a metastable configuration (that would give rise to large rejection rates).

In order to check that the simulation code is working properly, we have compared our simulation against known results for the scaling exponents of equilibrium quantities such as the radius of gyration and the end-to-end distance of the polymer. We have also evaluated the correlation time of these quantities, which plays an important role in the nonequilibrium situation (it sets the time scale for the polymer dynamics in shear flow).

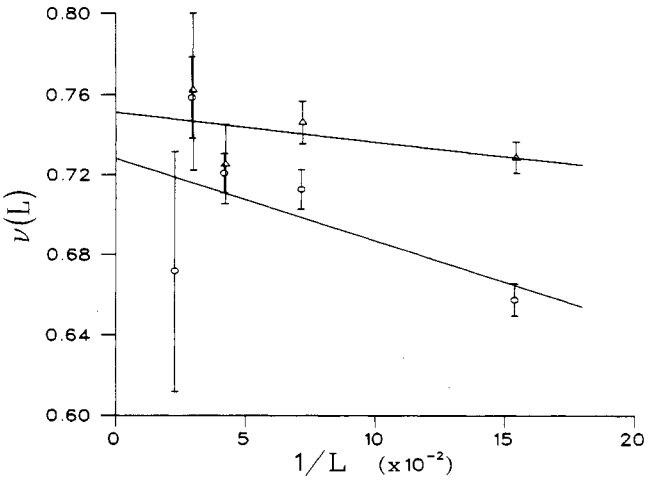

Figure 1. $\nu(L)$ versus $1/L$ for R_g (○) and R_{1n} (△).

The radius of gyration and the end-to-end distance are first calculated as functions of polymer length, $L = N - 1$. They are expected to depend on L as

$$R_{1n} \propto R_g \propto L^\nu \quad (3.1)$$

Owing to the relatively small values of N used in the simulation, we expect to obtain values of ν that have some residual dependence on L that is different for R_g and R_{1n}. In Figure 1 we plot the L-dependent values of $\nu(L)$, as a function of $1/L$. Least-squares fits to these points are also shown. In the asymptotic limit, $L \to \infty$, we obtain $\nu_{R_g} = 0.73 \pm 0.05$ and $\nu_{R_{1n}} = 0.75 \pm 0.04$, both consistent with the exact result 0.75. At finite values of L we also observe that $\nu_{R_{1n}}(L)$ is larger and less L-dependent than $\nu_{R_g}(L)$. This means that careful analysis of the data obtained from calculations on relatively small polymers, $5 \le N \le 50$, can give a reliable extrapolation to the asymptotic limit. The above applies particularly well to the calculation of the end-to-end distance and is somewhat less correct with regard to the radius of gyration. The later result is more strongly dependent on L because the calculation of R_g involves the positions of all the monomers and in that sense all the intrapolymer length scales, while only the positions of the end monomers enter the calculation of the end-to-end distance. The above observations are used in the next section where both the end-to-end distance and the radius of gyration are studied as functions of the position of the center of mass of a polymer confined to move between parallel walls. There we consider a polymer of 10 monomers for which we have measured (Figure 1) the equilibrium exponents $\nu_{R_{1n}}(10) \simeq 0.74$ and $\nu_{R_g}(10) \simeq 0.70$, e.g., values that are still close to the excluded-volume result 0.75. These values are far from the $\nu = 0.50 \pm 0.02$ exponent we obtain for both quantities in the absence of excluded-volume interactions, which shows that excluded-volume effects play an important role even for such short chains.

The correlation functions were studied for polymers of size $4 \le L \le 39$. The autocorrelation functions of both the end-to-end distance and the radius of gyration, without excluded-volume interactions, give the correlation times $\tau_{R_g} = \tau_{R_{1n}} = (0.50 \pm 0.02)T_0$, where $T_0 = L^{1+2\nu}/s^2$. In the presence of excluded-volume interactions, $\tau_{R_g} = \tau_{R_{1n}} = \tau = (0.35 \pm 0.02)T_0$. Note that T_0 with excluded volume is larger than the corresponding time without excluded volume, owing to a higher value of ν.

4. Shear Flow between Repulsive Boundaries

Consider a polymer of $N = 10$ monomers, restricted to move in the (x,y) plane between two hard walls parallel

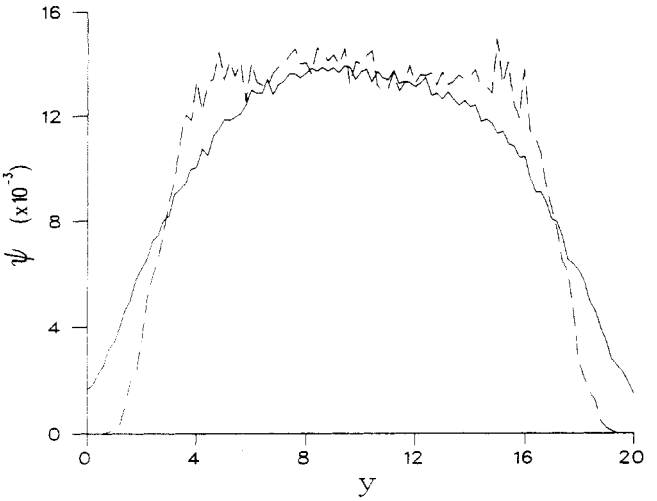

Figure 2. Distribution of monomers, Ψ_m (single line), and of centers of mass, Ψ_{cm} (dashed line), as a function of the distance from the left wall, y (no shear).

to the x axis. The left wall is located at $y_L = 0$, and the right wall is at $y_R = 20$. In fact, the distance between the walls is fixed at 21, but since a monomer has a finite radius, $b = 0.5$, the total accessible separation between the walls is 20. The choice of this particular separation is dictated by the need to satisfy two opposing demands: (1) Polymers located in the "bulk" region at the center of the flow channel should not interact with the wall. This condition is satisfied when $2R_g \ll y_R - y_L$. (2) The depletion region, which is roughly of polymer dimensions (R_g, in the zero shear case), is much smaller but not negligible with respect to the size of the bulk region. This ensures that equilibrium is achieved with respect to the slowest process in the problem (which is polymer diffusion transverse to the wall), for practically accessible simulation times. The spatial resolution is defined by dividing the separation between the boundaries into 100 equal intervals.

We calculate the normalized monomer (Ψ_m) and center of mass (Ψ_{cm}) distributions as a function of the distance from the wall, y. These distributions are plotted in Figure 2, for the case of excluded-volume interactions and no shear. While Ψ_m decreases faster than Ψ_{cm} as one starts to approach the wall, the situation is reversed closer to the wall where Ψ_{cm} decreases faster than Ψ_m.

We also study the dependence of the perpendicular and parallel (to the wall) components of the radius of gyration, $R_{g,pe}$ and $R_{g,pa}$, respectively, on the position of the center of mass of the polymer. The above quantities are plotted in parts a and b of Figure 3, for the case of excluded interactions and no shear flow. The main features observed in this case are as follows: (1) The effects of the boundaries are negligible in the bulk region away from the walls, i.e., $R_{g,pa} = R_{g,pe}$ (and similarly for the end-to-end distance, $R_{1n,pa} = R_{1n,pe}$), and the value of R_g (and of R_{1n}) is the same as in free space. (2) $R_{g,pa}$ (and $R_{1n,pa}$) increases, while $R_{g,pe}$ (and $R_{1n,pe}$) decreases as we approach the wall, in agreement with the intuitive expectation that the polymer becomes stretched and oriented parallel to the wall. Since the behavior of R_g and R_{1n} is qualitatively similar, from here on we omit the subscripts g and $1n$.

Near the walls R_{pe} decreases more strongly than R_{pa} increases, such that the area, $A = R_{pa}R_{pe}$, still decreases (Figure 3c). At the same time we find that the distance between nearest-neighboring monomers is independent of the distance from the wall, indicating that while the

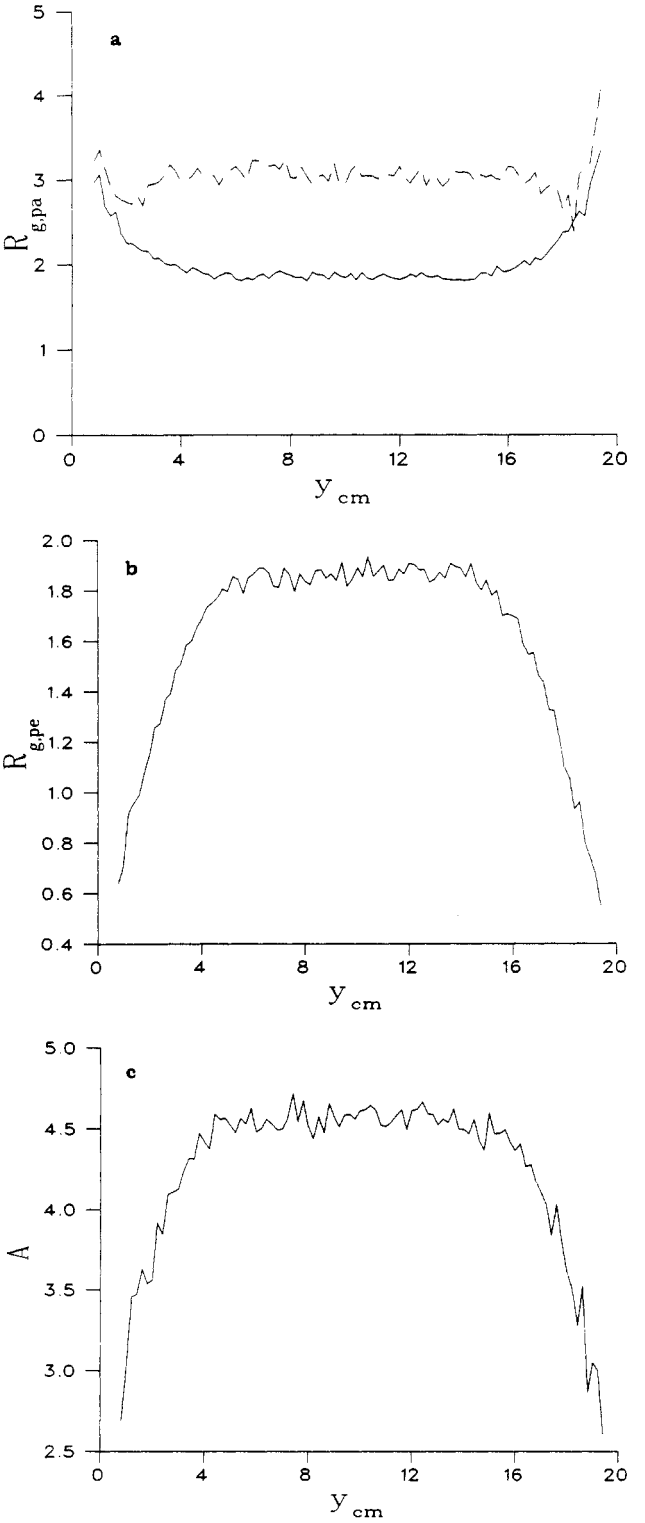

Figure 3. (a) $R_{g,pa}$ versus y_{cm}, without (single line) and with (dashed line) shear flow. (b) $R_{g,pe}$ versus y_{cm}, no shear. (c) $A = R_{g,pa}R_{g,pe}$ versus y_{cm}, no shear.

presence of the boundary has a large effect on the global conformation of the polymer, the small scales are not affected by it.

A simple shear flow is introduced such that the velocity field in the space between the walls is given by $v_x = gy$, where g is the shear rate (the magnitude of the velocity gradient). The simulation technique is analogous to that in the absence of shear; i.e., a monomer is chosen at random and its position is updated in the following manner: we pick a vector of fixed length s and random direction and add to its projection on the x axis a flow-

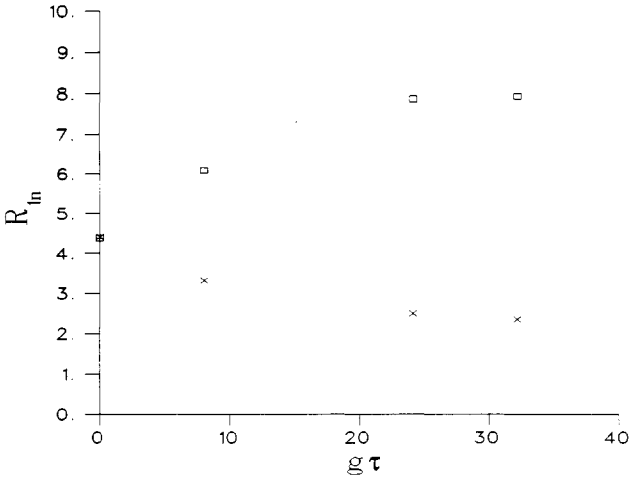

Figure 4. Bulk values of $R_{1n,pa}$ (□) and $R_{1n,pe}$ (×) versus $g\tau$.

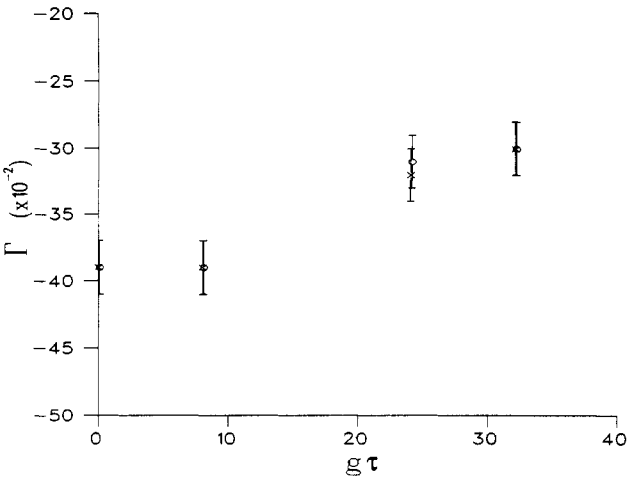

Figure 5. Total surface excess Γ_m (×) and Γ_{cm} (○) versus $g\tau$.

induced displacement $g(y - y_{cm})\,dt$. The y component of the random vector is not affected by the flow. The resulting vector is then added to the current position of the monomer, and the process is repeated N times during a time unit, $dt = 1$. Note that the above algorithm involves a first-order approximation (replacing differentials by differences) to the numerical integration of the equations of motion for the monomers in the presence of shear flow.

We now turn to study the distributions of monomers and center of mass as well as R_{pa} and R_{pe}, in the presence of excluded-volume interactions and shear flow. The main difference compared to the no-flow case is that the polymer is distorted and oriented along the flow axis, even in the central bulk region, resulting in smaller values of R_{pe} and larger values of R_{pa}. Very close to the wall, the polymer conformation is not affected by the flow and depends only upon the distance from the boundary. Further away from the wall, a transition zone is observed that separates the shear-dominated bulk region from the wall region in which the distortion is dominated by wall exclusion effects. The transition region moves close to the wall as the rate of shear is increased. This behavior is shown in Figure 3a where $R_{g,pa}$ is plotted as a function of the distance to the wall in presence of excluded-volume interactions and shear flow. Rather unexpectedly, a dip is observed in the transition region, which means that polymer extension/orientation has a minimum in this region. The behavior of the parallel and the perpendicular components to the end-to-end distance as a function of the dimensionless rate of shear ($g\tau$) is shown in Figure 4. The apparent saturation observed in both R_{pa} and R_{pe} in the limit of strong shear, $g\tau \geq 25$, may be taken as an indication that the polymer approaches full extension. Notice, however, that, for the largest shear rate, the extension is only about half of the maximum. Furthermore, calculation of the separation between nearest-neighboring monomers shows that it increases by less than 1% over its equilibrium value for the largest shear rates investigated and thus that the shear is still "weak" on a monomer scale.

Shear flow has only a small effect on the monomer and center of mass distributions, at least in the investigated range of shear rates. We may define the effective width, ξ_d, of the depletion layer as the distance of the appropriate distribution (Ψ_{cm} or Ψ_m) from the wall, at the point where it reaches a given fraction of its bulk value, and plot it as a function of $g\tau$. Unfortunately, the results appear to be sensitive to the shape of the distribution function in the region near the wall, where the statistics are relatively poor. In view of that above we choose to study the integrated properties of the density profiles, i.e., the total surface excesss Γ_m and Γ_{cm}, defined as

$$\Gamma_m(g\tau) = \int (\Psi_m(y) - \Psi_m{}^b)\,dy \qquad (4.1)$$

and

$$\Gamma_{cm}(g\tau) = \int (\Psi_{cm}(y) - \Psi_{cm}{}^b)\,dy \qquad (4.2)$$

where $\Psi_m{}^b$ and $\Psi_{cm}{}^b$ are the bulk values of the monomer and center of mass distribution functions, respectively, and where the integration is over the complete interval between the walls. A further advantage of considering the surface excess (or its negative, i.e., wall depletion) is that it has been studied experimentally, using the EWIF technique.[6] We find that both Γ_m and Γ_{cm} increase with the rate of shear (Figure 5), indicating that in the presence of shear flow the polymers move closer to the wall.

5. Discussion

We have investigated the behavior of two-dimensional polymers with excluded-volume interactions, near repulsive boundaries, both in equilibrium and in the presence of simple shear flow. The equilibrium properties of dilute polymer solutions near repulsive walls were previously studied only for the case of Gaussian chains in Θ solvents, where exact analytical results for the monomer distribution function are available.[9] Some of the considerations originally made for semidilute solutions in good solvents[10,11] apply equally well to the dilute case, provided that one replaces the bulk correlation length by the radius of gyration of the polymer. In particular, one expects that well inside the depletion region, i.e., for $b \ll y \ll R_g$, the distance to the wall, y, is the only relevant length scale in the problem and that, as a consequence, R_{pe} decreases linearly with polymer distance from the boundary, y_{cm}. This conclusion (and the associated increase of R_{pa}) is consistent with our observations, parts a and b of Figure 3.

The case of a dilute solution of elastic dumbbells without excluded volume, flowing through a narrow channel, has been considered by several investigators. However, as has been pointed out in connection with inhomogeneous (i.e., with position-dependent velocity gradients) flows,[3] most authors assume that the distribution function for the "beads" is separable, that is, can be expressed as a product of distribution functions for the center of mass and the relative coordinates. While this separa-

tion of coordinates is an exact property of the Rouse model in homogeneous space, the symmetry of the underlying equation is broken by the boundary conditions (the confining walls), even in the absence of flow. The breakdown of the separability assumption in the vicinity of the walls (even in equilibrium!) becomes evident when one examines the dependence of polymer conformations on the distance from the wall (parts a and b of Figure 3) and compares it to the assumption that the end-to-end distance of the dumbbell (i.e., the relative displacement of the beads) is independent of the position of its center of mass. Similar effects are observed in simple shear flow. The bulk region is strongly affected by shear, which induces increasingly large deformation of the polymers. Near the wall, the effect of shear-induced deformation is small compared to that of wall exclusion. As expected, the transition zone moves closer to the wall and the difference between the magnitudes of the distortion in both regions is reduced when the shear rate is increased (see Figure 3a). Notice, however, that the distortion and the orientation effects are different in the two cases: while wall exclusion distorts and orients the polymers parallel to the wall, the steady-state conformation of a polymer in two-dimensional shear flow is that of an elongated ellipsoid with the major axis oriented at a finite, shear-dependent angle to the direction of flow.[12] The polymer conformation becomes position independent only in the limit of infinite shear rates.

What happens to the polymer concentration profile in the presence of shear flow? A theoretical analysis of the problem of wall effects in unidirectional flow has been carried out for a dilute solution of elastic dumbbells, and it has been concluded that the shear does not affect the monomer distribution near the wall.[4] We believe that the difference between this conclusion and our results can be traced back to the choice of a particular solution for the joint probability distribution of the positions of the beads that depends only on the relative coordinates and does not involve the center of mass position.[4]

Very recently, an EWIF study of the polymer concentration profile in shear reported that the surface excess decreases with the rate of shear.[6] This observation contradicts our results, and we can only speculate about the reasons for the discrepancy. If theory is at fault, it is conceivable that the observed effect is caused by hydrodynamic interactions that are not taken into account in our work. While these interactions may be screened by the presence of a wall, leading to a decrease of the polymer diffusion coefficient near the boundary, it is not clear in what way this "slowing down" affects the polymer distribution in the depletion layer. Another possibility involves the fact that the flow field in the experiment is a plane Poiseuille (rather than simple shear) flow in which the velocity gradient is a linearly decreasing function of the distance from the wall. Although it is known that the inhomogeneity of the flow may affect the polymer concentration profile, it is believed that the above applies only to curvilinear flows in which the direction, as well as the magnitude, of the velocity gradients changes with position and that the effect does not occur in unidirectional flows.[2,3] On the experimental side, one has to rule out the possibility of polymer adsorption on the walls of the flow device. High shear rates are known to induce desorption (and possibly degradation) of the polymers from the walls,[13,14] thus leading to the decrease of the polymer concentration in the depletion layer that is consistent with the observed effect. While we cannot comment on whether the above mechanism is present in the EWIF experiments, we will discuss the model proposed by Ausserré et al. and compare it with our findings.

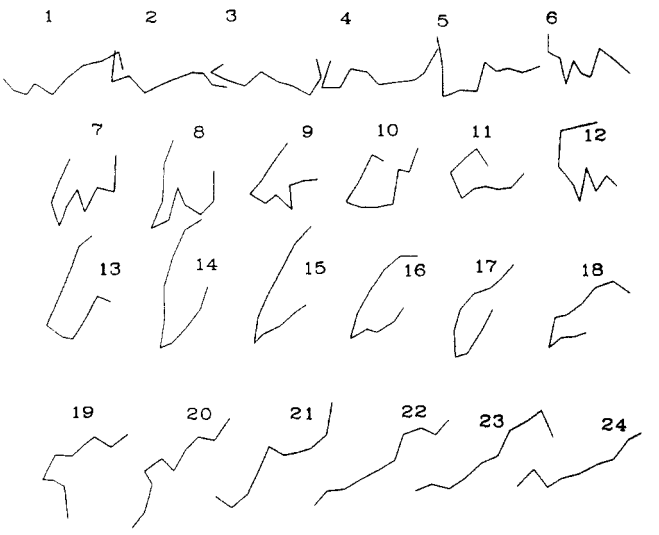

Figure 6. Sequence of polymer configurations in strong shear flow, $g\tau = 32.11$, sampled during a correlation time, τ.

Wall depletion results from the fact that many polymer configurations are prohibited by the presence of a repulsive boundary. Since in steady state the polymer becomes distorted and oriented along the flow and since its transverse dimensions decrease with the shear rate, the intuitive expectation is that, in the presence of shear flow, polymers approach the wall more closely than in equilibrium. In order to explain their observations, Ausserré et al. introduce an interesting idea that involves the dynamics of fluctuations about the steady state. They assume that the polymer (xanthan) can be thought of as a rigid rod that rotates owing to the combined effects of the frictional force exerted by the shear flow and the random Brownian force. When the rod is oriented at a sufficiently large angle to the flow axis, in the limit of strong shear ($g\tau \gg 1$) the flow-induced moment, which is proportional to the projection of the rod on the y axis, dominates over that of the random force. As the rod rotates to smaller angles, the relative magnitude of the deterministic force goes down, such that, at angles smaller than the critical one (θ_{cr}), the Brownian forces dominate. Thus, at an arbitrary shear rate g, there exists an angle $\theta_{cr}(g)$ that divides the space into shear flow and Brownian motion dominated regions. Since the size of the Brownian sector goes down as the shear rate is increased, the rod finds it increasingly easier to diffuse out of this sector and spends more time rotating through the shear-dominated sector. One concludes that the frequency of collisions with the wall (and hence, the number of forbidden configurations) goes up with the shear rate, resulting in an increased wall depletion. The authors emphasize that the proposed mechanism applies only to rigid rods and that flexible polymers may behave differently.

In order to test whether the above model applies to flexible polymers, we study the polymer configurations in strong shear flow ($g\tau = 32.11$). A typical sequence of configurations sampled during a single correlation time, τ, is plotted in Figure 6. Note that there is a strong coupling between polymer rotation and deformation. The polymer reaches maximum elongation at a finite angle with respect to the flow direction, and when Brownian forces rotate it away from this angle, it tends to fold and assumes a relatively compact conformation. Thus, unlike in the rigid rod case, configurations in which the polymer is stretched perpendicular to the axis of maximal

extension are increasingly suppressed at higher shear rates. The conclusion that shear decreases the number of configurations in which the polymer would feel the presence of the wall is consistent with our observation of shear-induced enhancement of the surface excess Γ.

Acknowledgment. We are indebted to D. Ausserré, H. Hervet, and Y. Kantor for many useful discussions and thank the reviewers for very helpful comments. Y.R. thanks P.-G. de Gennes and J. Prost for the hospitality he received during his stay at the Laboratoire de la Matière Condensée of the Collège de France and at the ESPCI, where this work was started. This research was supported by U.S.–Israel Binational Science Foundation Grant No. 87-00134 and by DARPA (through the La Jolla Institute).

References and Notes

(1) Bird, R. B.; Hassager, O.; Armstrong, R. C.; Curtis, C. F. *Dynamics of Polymeric Liquids*; Wiley: New York, 1977.
(2) Aubert, J. H.; Tirrell, M. *J. Chem. Phys.* **1980**, *72*, 2694.
(3) Brunn, P. O. *Physica D* **1986**, *20*, 403.
(4) Brunn, P. O. *J. Rheol.* **1985**, *29*, 859.
(5) Rondelez, F.; Ausserré, D.; Hervet, H. *Annu. Rev. Phys. Chem.* **1987**, *38*, 317.
(6) Ausserré, D.; Edwards, J.; Lecourtier, J.; Hervet, H.; Rondelez, F. Hydrodynamic Thickening of Depletion Layers in Polymer Solutions. Submitted for publication in *Phys. Rev. Lett.*
(7) Kantor, Y.; Kardar, M.; Nelson, D. R. *Phys. Rev. A* **1987**, *35*, 3056.
(8) Ceperley, D.; Kalos, M. H.; Lebowitz, J. L. *Phys. Rev. Lett.* **1978**, *41*, 313.
(9) Casassa, E. F. *Macromolecules* **1984**, *17*, 601.
(10) Joanny, J. F.; Leibler, L.; de Gennes, P.-G. *J. Polym. Sci., Polym. Phys. Ed.* **1979**, *17*, 1073.
(11) de Gennes, P.-G. *Macromolecules* **1981**, *14*, 1637.
(12) Johnson, J. A. Y. *Macromolecules* **1987**, *20*, 103.
(13) Cohen, Y.; Metzner, A. B. *Macromolecules* **1982**, *15*, 1425.
(14) Lee, J. J.; Fuller, G. G. *Macromolecules* **1984**, *17*, 375.

The Interplay between Geometric and Electronic Structures in Polyisothianaphthene, Polyisonaphthothiophene, Polythieno(3,4-*b*)pyrazine, and Polythieno(3,4-*b*)quinoxaline

Kasinath Nayak and Dennis S. Marynick*

Department of Chemistry, Box 19065, The University of Texas at Arlington, Arlington, Texas 76019. *Received July 28, 1989; Revised Manuscript Received October 24, 1989*

ABSTRACT: PRDDO and ab initio molecular orbital calculations are employed to show that polyisothianaphthene and polyisonaphthothiophene are nonplanar polymers in their aromatic forms, due to steric interactions between the sulfur and hydrogen atoms from adjacent monomeric units; however, the planar quinoid form of polyisothianaphthene is calculated to be ~2 kcal/mol more stable than the aromatic nonplanar form. A simple procedure is introduced for extrapolating the conformational energetics calculated from oligomers to the infinite polymeric system. Similar calculations show that polythieno(3,4-*b*)pyrazine and polythieno(3,4-*b*)quinoxaline are perfectly planar systems in both the aromatic and quinoid forms. The extended Hückel technique is used to evaluate the electronic properties of both the aromatic and quinoid forms of these polymers. The band gaps obtained for the quinoid structure of these polymers are in good agreement with the experimental and other theoretical findings. These results have important implications for the design of new conducting polymers.

Introduction

Among electrically conducting polymers, polythiophenes have emerged as versatile conducting materials upon redox doping.[1] Substitution on the carbons at the β-positions has led to new polymers that are solution processible and others in which optical properties can be enhanced.[2] The "nonclassical" polythiophenes, polyisothianaphthene (PITN), and polyisonaphthothiophene (polynaphtho[2,3-*c*]thiophene) (PINT), whose monomers were initially prepared by Cava et al.,[3,4] are of particular interest, since both experimental[5–10] and theoretical[11–13] work suggest that these systems have very small or even vanishing band gaps. From the theoretical perspective, a number of studies[11–17] have appeared leading to a controversy concerning the relative energies of the aromatic and quinoid forms of polythiophene and its derivatives.

Isothianaphthene (ITN) can be viewed as a thiophene ring on which a benzene ring has been fused along the C_β–C_β bond. Wudl et al.[5–10] have successfully synthesized PITN and have reported the reduction in the energy gap of PITN to about half that of the parent polythiophene (E_g(PT) – E_g(PITN) = 1 eV). These polymers may assume two distinctly different electronic structures, commonly referred to as the "aromatic" and "quinoid" forms, as shown below. Brédas et al.[11–13] have also

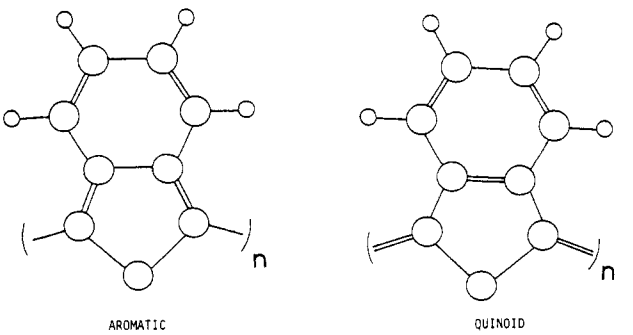

reported theoretical calculations that suggest a very small

0024-9297/90/2223-2237$02.50/0